The effect of uniaxial pressure on the magnetic anomalies of the heavy-fermion metamagnet $CeRu_2Si_2$

S. R. Saha, H. Sugawara, T. Namiki, Y. Aoki, and H. Sato
Department of Physics, Graduate School of Science, Tokyo Metropolitan University, Minami-Ohsawa 1-1, Hachioji, Tokyo 192-0397, Japan
(Dated: February 1, 2008)

The effect of uniaxial pressure (P_u) on the magnetic susceptibility (χ), magnetization (M), and magnetoresistance (MR) of the heavy-fermion metamagnet $CeRu_2Si_2$ has been investigated. For the magnetic field along the tetragonal c axis, it is found that characteristic physical quantities, i.e., the temperature of the susceptibility maximum ($T_{\max}$), the pagamagnetic Weiss temperature (Θ_p), $1/\chi$ at 2 K, and the magnetic field of the metamagnetic anomaly (H_M), scale approximately linearly with P_u, indicating that all the quantities are related to the same energy scale, probably of the Kondo temperature. The increase (decrease) of the quantities for $P_u \parallel c$ axis ($P_u \parallel a$ axis) can be attributed to a decrease (increase) in the nearest Ce-Ru distance. Consistently in MR and χ, we observed a sign that the anisotropic nature of the hybridization, which is believed to play an important role in the metamagnetic anomaly, can be controlled by applying the uniaxial pressure.

PACS numbers: 75.20.Hr, 71.27.+a, 74.62.Fj

I. INTRODUCTION

The compound, $CeRu_2Si_2$, crystallizing in the tetragonal $ThCr_2Si_2$-type structure, is one of the most intensively studied and best characterized systems among the heavy-fermion compounds.[1] The reason is that apart from a large electronic specific-heat coefficient $\gamma \sim 360$ mJ/mol K^2 in zero field,[2,3] there is an abrupt nonlinear increase of magnetization, the so called metamagnetic anomaly (MA) from a paramagnetic ground state, around an external magnetic field of $H_M \sim 80$ kOe (Ref. 1) applied only along the c axis of the tetragonal structure below 15 K. Not only the magnetization process but also many other physical properties have been reported to be anomalous in this field region around H_M.[3,4,5,6]

The origin of the anomaly is still a matter of debate, despite intensive investigations. The de Haas-van Alphen effect studies have shown that both the Fermi surface and the effective mass change considerably around H_M, suggesting a change of $4f$-electron character from itinerance in the low-field state to localization in the high-field state.[4] In contrast, low-temperature magnetization measurements[5] suggest that the low-field state is continuously connected to the high-field state across H_M. Moreover, a peak observed in the Hall resistivity at $H = H_M$ disappears on approaching $T = 0$, suggesting no abrupt change in the Fermi surface.[6] Reports of hydrostatic pressure experiments[7,8] reveal that the volume reduction enhances the characteristic energy of the quasiparticle system and leads to a drastic shift of H_M to higher fields. From this large effect of pressure a very large electronic Grüneisen parameter ~ 185 Mbar^{-1} has been inferred. The anisotropic hybridization between $4f$ and conduction electrons leading to an anomalous peak in the quasiparticle density-of-states (DOS) is argued to play an important role in the MA; the MA appears when the peak crosses the Fermi level at high magnetic fields.[3,9] However, no direct evidence of the anisotropic hybridization effect can be obtained from hydrostatic pressure experiments. The uniaxial-pressure experiment has the potential for providing useful information on anisotropic hybridization. In view of these reasons, we have investigated the effect of uniaxial pressure in $CeRu_2Si_2$ with magnetic and transport experiments.

II. EXPERIMENT

Single crystals of $CeRu_2Si_2$ were grown by the Czochralski pulling method in a tetra-arc furnace with an argon atmosphere. The single crystalline nature was confirmed by back-reflection-Laue techniques. The high quality of the single crystal was inferred from the residual resistivity ratio ≥ 110. Electrical resistivity and magnetoresistance were measured by the standard dc four probe method using a computer-controlled current source and nanovoltmeter (182 Keithley), using a top-loading ^{3}He cryostat equipped with a 160 kOe superconducting magnet (Oxford Instruments Co., Ltd.). The electrical contacts of Ag current leads were affixed to the sample by indium soldering. Au wires of 80-μmϕ were spotwelded to the sample as voltage leads. Uniaxial pressures were generated by using a piston-cylinder-type CuBe pressure cell for transport experiments, recently designed and constructed by us[10], so as to suit the above cryostat. Single-crystal samples (typical dimensions: $\sim$ 0.7 x 1 x 2 mm^3) were sandwiched between two disc-shaped ZrO_2 plates, which provided the electrical isolation. A Nitflon tape of 0.08-mm thickness was placed between the sample and ZrO_2 plates in order to prevent the breaking of the sample due to its surface roughness under pressure, if any. Uniaxial pressures were

applied on a ZrO_2 ball, placed inside a ring-shaped guide on the ZrO_2 plate above the sample, which prevented any rotation of the sample under pressure. Uniaxial pressures produced on the sample at low temperatures were calibrated by measuring the superconducting transition temperature of Sn placed in the cell by an induction method. Magnetic properties were measured by a commercial superconducting quantum interference device (SQUID) magnetometer. Uniaxial pressures parallel to the magnetic fields were generated by using a modified version of the SQUID-pressure cell reported by Uwatoko *et al.*[11] Uniaxial pressures produced on the rectangular shaped single crystal ($\sim$ 1.5 x 1.5 x 2 mm^3) at low temperatures were calibrated by measuring the Meissner effect of a small piece of Pb, placed in the pressure cell. The known pressure dependences of the superconducting transition temperature of Sn (Ref. 12) (for transport measurements) and Pb (Ref. 13) were used for these purposes. Uniaxial pressures perpendicular to the magnetic fields were generated by a uniaxial-pressure cell recently designed and constructed by us[10]. In this case, the uniaxial pressures were determined at room temperature by the absolute value of force applied on the sample. The total magnetization of the sample and the uniaxial-pressure cell were measured by SQUID magnetometer and the magnetization of the uniaxial-pressure cell, though small ($1 - 10\%$), were subtracted from the total magnetization to obtain the precise value of the sample magnetization.

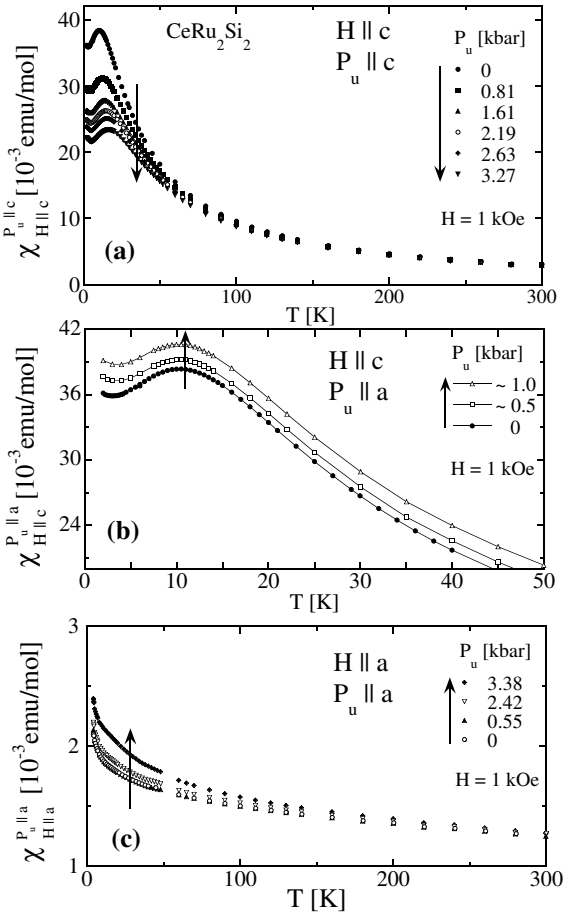

FIG. 1: Temperature dependence of magnetic susceptibility (χ) in $CeRu_2Si_2$ under uniaxial pressure (P_u). (a) $\chi^{P_u\|c}_{H\|c}(T)$ for P_u applied parallel with the magnetic field (H) along the tetragonal c axis. (b) $\chi^{P_u\|a}_{H\|c}(T)$ for P_u along the a axis and H along the c axis. (c) $\chi^{P_u\|a}_{H\|a}$ for P_u and H along the a axis. The arrows indicate the change of χ with increasing P_u.

III. EXPERIMENTAL RESULTS

Figure 1 shows the effect of uniaxial pressure on the temperature dependence of magnetic susceptibility $\chi(T)$ in $CeRu_2Si_2$; Fig. 1(a) is for $P_u \parallel H \parallel c$ axis, Fig. 1(b) is for $P_u \parallel a$ and $H \parallel c$ axis, and Fig. 1(c) is for $P_u \parallel H \parallel a$ axis. At ambient pressure, the magnetic susceptibility is strongly anisotropic depending on whether H is applied parallel or perpendicular to the tetragonal c axis. $\chi_{H\|c}(T)$ obeys the Curie-Weiss law above $\sim$ 70 K and then shows a maximum at a temperature $T_{\rm max} \simeq 10$ K, which is considered to provide a measure of the Kondo temperature $T_{\rm K}$. $\chi_{H\|a}(T)$ also follows the Curie-Weiss law above 100 K, and it exhibits much smaller values than $\chi_{H\|c}(T)$, without showing any maximum. The anisotropy ratio $\chi_{H\|c}(T)/\chi_{H\|a}(T)$ increases largely with decreasing temperatures. These behaviors at ambient pressure are consistent with those reported before[7]. When the uniaxial pressure of $P_u \parallel c$ axis is applied, $\chi^{P_u\|c}_{H\|c}$ for $H \parallel c$-axis is largely suppressed at low temperatures with increasing P_u, though the effect of P_u is small at higher temperature ($\geq$100 K). $T_{\rm max}$ shifts to higher temperatures with increasing P_u, i.e., $T_{\rm max} \simeq 16.5$ K at $P_u \simeq 3.27$ kbar. The pressure dependence is almost similar to that under hydrostatic pressure (P_h) repoted in Refs. 7 and 8. By contrast, when P_u is applied perpendicular to the magnetic field, i.e., $P_u \parallel a$ axis, $\chi^{P_u\|a}_{H\|c}$ at low temperatures is enhanced and $T_{\rm max}$ is slightly suppressed [see Fig. 1(b)]. On the other hand for $H \parallel a$ axis, $\chi^{P_u\|a}_{H\|a}$ slightly increases at low temperatures with $P_u \parallel a$ axis [see Fig. 1(c)]. This increase of $\chi^{P_u\|a}_{H\|a}$ is also in contrast to the decrease of $\chi^{P_h}_{H\|a}$ under hydrostatic pressure[7]. In the case of $P_u \parallel c$ axis, $\chi^{P_u\|c}_{H\|a}$ weakly enhances at low temperatures with P_u (not shown); it is difficult to separate accurately the background contribution from the pressure cell which is comparable to the sample magnetization for $H \parallel a$ axis.

Figure 2 shows the effect of uniaxial pressure on the magnetic-field dependence of isothermal (at 2 K) magnetization $M(H)$ in $CeRu_2Si_2$. The ambient pressure data are consistent with those reported before[7]. For $H \parallel c$ axis, a positive curvature of $M^{P_u\|c}_{H\|c}(H)$ is observed as a

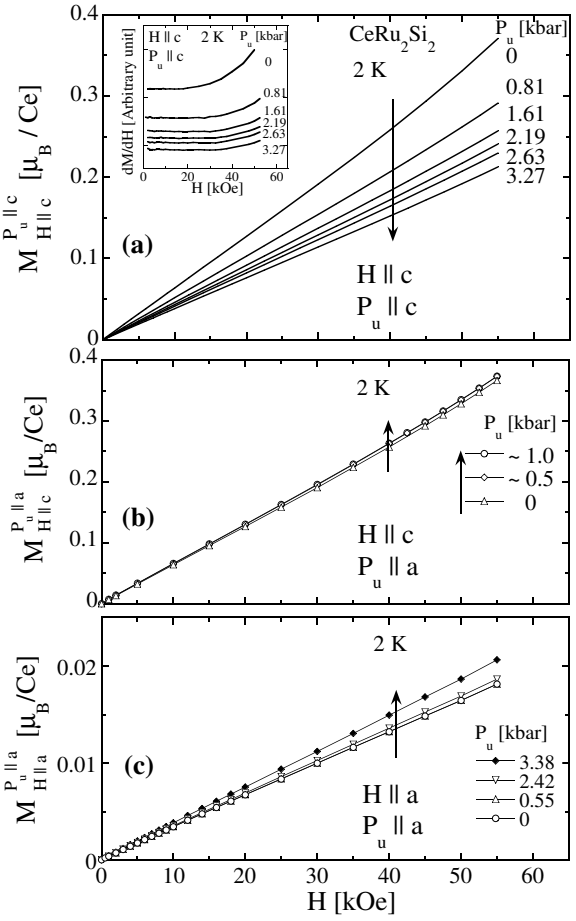

FIG. 2: Magnetic-field dependence of isothermal magnetization $M(H)$ in $CeRu_2Si_2$ under uniaxial pressure at 2 K. (a) $M^{P_u\|c}_{H\|c}(H)$ for P_u applied parallel with the magnetic field along the tetragonal c axis. (b) $M^{P_u\|a}_{H\|c}(H)$ for P_u along the a axis and H along the c axis. (c) $M^{P_u\|a}_{H\|a}(H)$ for P_u and H along the a axis. The arrows indicate the change of M with increasing P_u. The solid lines are guides to the eyes.

precursor to the metamagnetic anomaly at $H_M \simeq 80$ kOe at ambient pressure. Under $P_u \parallel c$ axis, $M^{P_u\|c}_{H\|c}$ up to 55 kOe drastically decreases [see Fig. 2(a)] and the curvature $\partial M^{P_u\|c}_{H\|c}/\partial H$ at 55 kOe is also largely suppressed with increasing P_u as shown in the inset of Fig. 2(a). These facts indicate a shift of the metamagnetic anomaly to higher magnetic fields by $P_u \parallel c$ axis; actually, this is confirmed by the magnetoresistance measurement (see Fig. 3). This effect of $P_u \parallel c$ axis on the isothermal $M^{P_u\|c}_{H\|c}(H)$ is similar to the effect of P_h on the isothermal magnetization $M^{P_h}_{H\|c}(H)$ reported in Ref. 7, where $M^{P_h}_{H\|c}$ and $\partial M^{P_h}_{H\|c}/\partial H$ also drastically decrease with increasing P_h. By contrast, under $P_u \parallel a$ axis, $M^{P_u\|a}_{H\|c}$ is enhanced [see Fig. 2(b)] and the $\partial M^{P_u\|a}_{H\|c}/\partial H$ at 55 kOe is also weakly enhanced. On the other hand for $H \parallel a$ axis, $P_u \parallel a$ axis enhances $M^{P\|a}_{H\|a}$ [see Fig. 2(c)]. This increase of $M^{P_u\|a}_{H\|a}$ is in sharp contrast to the decrease of $M^{P_h}_{H\|a}$ under hydrostatic pressure[7].

In order to see the effect of uniaxial pressure on the MA, we have measured the magnetoresistance (MR) up to 140 kOe under P_u. Figure 3(a) shows the effect of $P_u \parallel c$ axis on the magnetic field dependence of the transverse magnetoresistance, i.e., H along the c axis and the current J along the a axis. The data for $P_u \sim 0$ kbar are in close agreement with that reported in Ref. 8. The resistivity increases with magnetic fields and then shows a maximum or peak at $H_{\max} \simeq 83$ kOe. The MA manifests

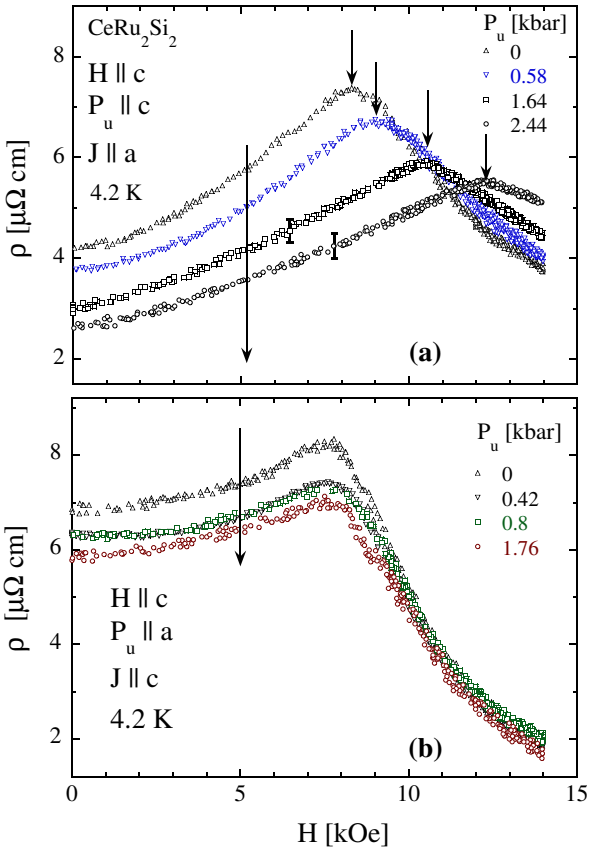

FIG. 3: Magnetoresistance (MR) in $CeRu_2Si_2$ at 4.2 K under uniaxial pressure P_u (a) for $P_u \parallel c$ axis ($0 \le P_u \le 2.44$ kbar) and transverse geometry ($H \parallel c$ axis, $J \parallel a$ axis). The short arrows indicate the magnetic fields H_M where the maximum in $\rho(H)$ occurs, reflecting the metamagnetic anomaly. The error bars are put in the vertical axis after smoothing the scattered data points at higher pressures due to deterioration of the spotweld of the voltage leads. (b) for $P_u \parallel a$ axis ($0 \le P_u \le 1.76$ kbar) and longitudinal geometry ($H \parallel J \parallel c$ axis). The long arrows indicate the decrease of ρ below H_M with increasing P_u in both figures.

itself in this peak at $H_{\rm max}$ ($\equiv H_M$). With increasing P_u, the resistivity below H_M decreases and the peak shifts to higher H as marked by vertical arrows. These behaviors are similar to those under hydrostatic pressure reported in Ref. 8, though there are small quantitative differences. The most significant differences are that the absolute value of ρ at the peak (at H_M) decreases and the shape of the peak broadens with increasing $P_u \parallel c$-axis, while these remain almost unchanged for all values of P_h. These behaviors under P_h have been ascribed to the implication that the quasiparticle DOS always reaches the same critical value at H_M[8]. This conclusion was made by taking into account the following facts: H_M depends on pressure but it depends only slightly on temperature. At all values of P_h, the ρ at $H = H_M$ of the corresponding P_h shows almost the same temperature dependence. Therefore, the slope of each $\rho(T)$ curve of $H = H_M$, which gives an estimation about the DOS at $H = H_M$, remains unchanged with P_h[8]. Based on the same model, in the present case under $P_u \parallel c$ axis, the decrease and broadening of the peak at H_M may indicate a change of the quasiparticle DOS near the metamagnetic anomaly at H_M with increasing $P_u \parallel c$ axis. However, measurements at low temperatures are necessary in order to reach a decisive conclusion.

Figure 3(b) shows the effect of $P_u \parallel a$ axis on the magnetic field dependence of longitudinal magnetoresistance, i.e., H along c axis and J along the a axis. The application of $P_u \parallel a$ axis is very risky, since large cracks easily develop into the samples. Some samples were completely separated into pieces in the c plane under pressure, making the measurement impossible several times. The ambient pressure ($P_u \sim 0$) data cannot be compared with that of Ref. 8, since there is no data for this geometry, however, the data are consistent in nature to the reported longitudinal MR at lower temperatures by Kambe *et al.*[6]. The data for $P_u \sim 0$ and 0.8 kbar have been taken on the same sample piece, but for $P_u \sim 0.4$ and 1.76 kbar the data have been taken on two different sample pieces, although all the pieces were cut from the adjacent part of the same crystal. The results shown in Fig. 3(b) indicate that the sample dependence is minor at least for these three pieces. With increasing $P_u \parallel a$ axis, the resistivity decreases for all H, though the change in ρ above H_M is smaller than that below H_M. The magnetoresistance peak at H_M (~ 80 kOe at ambient pressure), manifesting the metamagnetic anomaly, changes only slightly with increasing P_u. There is a slight decreasing tendency of H_M [see Fig. 4(c)] with increasing P_u, although it is difficult to determine accurately the rate $\Delta H_M/\Delta P_u$ due to its extremely small change relative to the experimental accuracy.

Figure 4(a) shows the dependence of $T_{\rm max}$ in $\chi_{H\parallel c}(T)$ on P_u along with that on P_h reported by Voiron *et al.*[7]. $T_{\rm max}$ is enhanced with $P_u \parallel c$ axis as $\mathrm{d}T_{\rm max}/\mathrm{d}P_u \simeq 1.85 \pm 0.1$ K/kbar which is close to the rate $\mathrm{d}T_{\rm max}/\mathrm{d}P_h \simeq 2.5$ K/kbar for the P_h reported in Refs. 7 and 8. The absolute value of the paramagnetic Weiss temperature $\Theta_{\rm p}$, determined from the linear region of the inverse of $\chi^{P_u\parallel c}_{H\parallel c}(T)$ plot (below 100 K) shown in the inset of Figure 4(a), is also found to increase with $P_u \parallel c$ axis as shown in the same figure. The negative sign of Θ_p can be attributed to Kondo correlations. On the other hand, $T_{\rm max}$ is suppressed by $P_u \parallel a$ axis. Fig. 4(b) shows the P_u dependence of $1/\chi_{H\parallel c}$ at $T = 2$ K, which is enhanced and suppressed by $P_u \parallel c$ axis and $P_u \parallel a$ axis, respectively. Note that the low-temperature value of χ^{-1} is proportional to the Kondo temperature T_K in the Fermi-liquid regime. Figure 4(c) shows the P_u dependence of H_M in MR. H_M strongly increases by $P_u \parallel c$ axis as $\Delta H_M/\Delta P_u \sim 17 \pm 2$ kOe/kbar which is close to the rate ~ 20 kOe/kbar under

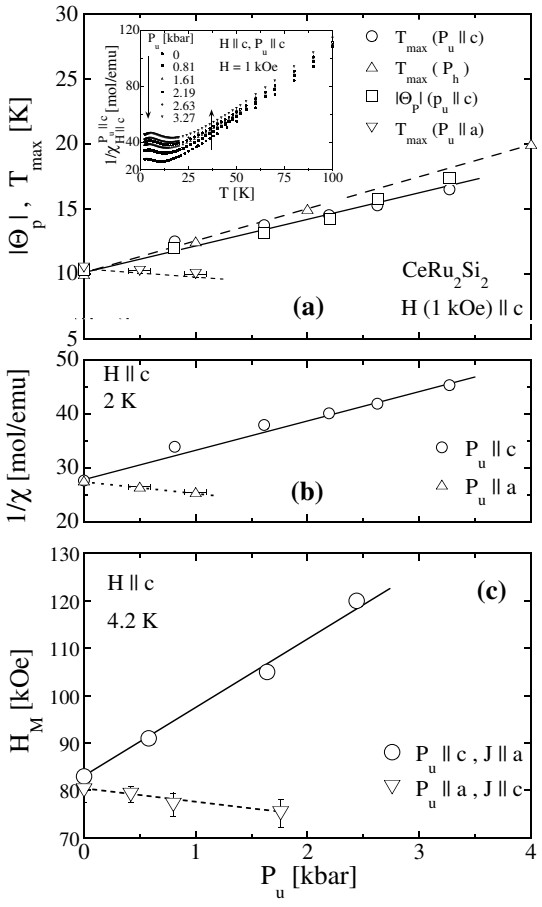

FIG. 4: (a) Uniaxial pressure dependence of $T_{\rm max}$ in $\chi^{P_u\parallel c}_{H\parallel c}$ and the absolute value of the paramagnetic Weiss temperature Θ_p, estimated from the linear region of the inverse $\chi^{P_u\parallel c}_{H\parallel c}$ plot below 100 K shown in the inset; the evolution of $T_{\rm max}$ under P_h reproduced from the report by Voiron *et al.* (Ref. 7) is also ploted at the same time. (b) Uniaxial-pressure dependence of the inverse $\chi^{P_u\parallel c}_{H\parallel c}$ and $\chi^{P_u\parallel a}_{H\parallel c}$ at 2 K. (c) Uniaxial pressure dependence of H_M in the transverse ($H \parallel c$ axis, $J \parallel a$ axis) magnetoresistance under $P_u \parallel c$-axis and longitudinal ($H \parallel J \parallel c$ axis) magnetoresistance under $P_u \parallel a$ axis in $CeRu_2Si_2$. The solid and broken lines are guides to eyes.

P_h[8], while H_M slightly decreases by $P_u \parallel a$ axis.
Mignot *et al.*[8] have shown that the hydrostatic pressure dependence of $T_{\max}$, $\chi^{-1}_{T\simeq 0}$, and H_M show a scaling behavior. A similar plot has been made as a function of P_u, where all the quantities $T_{\max}$, $\Theta_{\rm p}$, $\chi^{-1}_{T\simeq 0}$, and H_M are normalized by their ambient pressure values as shown in Fig. 5. $T_{\max}$ under P_h normalized by the ambient pressure value is also plotted for comparison. It is clear that all the quantities scale roughly falling on the same lines. This fact indicates, similar to the case of hydrostatic pressure[8], an existence of a single energy parameter that determines the low temperature properties controlled by P_u. Considering that both the low-temperature value of $\chi^{-1}_{T\simeq 0}$ in the Fermi-liquid regime and Θ_p are proportional to the Kondo temperature T_K, the observed scaling strongly indicates that both $T_{\max}$ and H_M are also related to the Kondo effect. The strong increase (weak decrease) of all the quantities indicates the strong enhancement (the weak suppression) of hybridization between conduction and f electrons under $P_u \parallel c$ axis ($P_u \parallel a$ axis). In other words, T_K is strongly increased by $P_u \parallel c$ axis, while it is decreased by $P_u \parallel a$ axis.

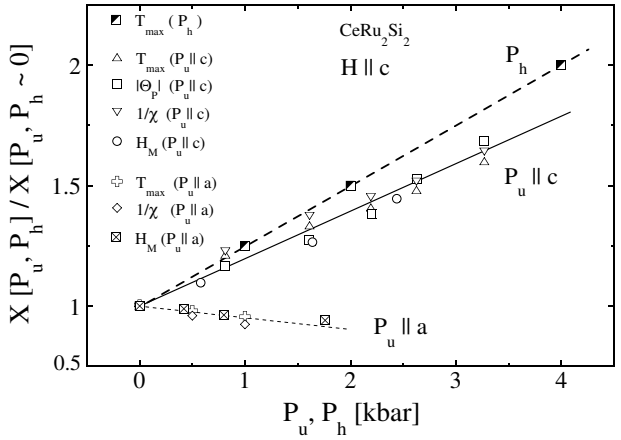

FIG. 5: $T_{\max}$, Θ_p, $\chi^{-1}_{T\simeq 0}$, and H_M normalized by the ambient pressure value of each parameter as a function of P_u. Solid lines are drawn to show that all the normalized parameters (X) for the same uniaxial-pressure geometry fall roughly on the same line. $T_{\max}$ under P_h, reported in Ref. 7 normalized by the ambient pressure value is also ploted at the same time. The solid and broken lines are guides to the eyes.

IV. DISCUSSIONS

In the previous section, we have shown that the effect of uniaxial pressures on the transport and magnetic properties is quite anisotropic. Especially, a qualitatively opposite effect on T_K is observed between $P_u \parallel a$ axis and $P_u \parallel c$ axis configurations. In order to understand this, we estimate the movement of the surrounding ions relative to the Ce ions due to the uniaxial pressures, taking into account the elastic properties reported to date.
The elastic constants of $CeRu_2Si_2$ at 300 K have been reported by Weber[14], i.e., $C_{11} \simeq 2.145$, $C_{12} \simeq 0.67$, $C_{33} \simeq 1.215$, and $C_{13} \simeq 0.806$ Mbar. We use these values since the low temperature values are not complete; no data are available at low temperatures for C_{12} in Ref. 14. Note that the temperature dependence of these quantities does not qualitatively affect our consequence shown below. Using these values, the linear compressibilities along the principal crystalline directions are then calculated as $\kappa_a \equiv -[\Delta a/\Delta P_u]/a \simeq 0.63$ Mbar^{-1} and $\kappa_c \equiv -[\Delta c/\Delta P_u]/c \simeq 1.33$ Mbar^{-1} for the a axis and c axis, respectively. Three Poisson ratios are also calculated. Under $P_u \parallel a$ axis, the Poisson ratio along the c axis is $\nu_c^{P_u \parallel a} \simeq 0.608$, while that along another a axis is $\nu_a^{P_u \parallel a} \simeq 0.084$. On the other hand under $P_u \parallel c$ axis, the Poisson ratio is $\nu_a^{P_u \parallel c} \simeq 0.286$. The values are quite anisotropic, i.e., for P_u along the a axis, the elongation along the c axis is more than seven times larger than that along the other a axis.
It is believed that the hybridization between f states and conduction electrons in $CeRu_2Si_2$ is mainly governed by d-f hybridization[15]. The band-structure calculation[16] indicates that there are five bands crossing the Fermi level (four hole sheets and one electron sheet), and they consist dominantly of the Ce $4f$ and the Ru $4d$ components. Actually, the nearest atom from Ce ions is Ru, suggesting strong hybridization between $4f$ and $4d$ electrons. Using the same lattice constants and atomic positions used in Ref. 16, the distances between the nearest neighbor Ce-Ru are calculated as a function of uniaxial pressure. The results are shown in Fig. 6. For the cases of applied uniaxial pressure along the c-axis and hydrostatic pressure, Ce-Ru distance $d_{\rm Ce-Ru}$ (= 3.224 Å at ambient pressure) decreases. On the other hand for the uniaxial pressure along the a axis, the crystal symmetry decreases from tetragonal to orthorhombic and two unequivalent $d_{\rm Ce-Ru}$ appear, however, the average value of $d_{\rm Ce-Ru}$ weakly increases. In the former case, decreasing $d_{\rm Ce-Ru}$ should cause an increase of the d-f exchange interaction J_{df}, and also an increase of T_K, which depends on J_{df} essentially as $\propto \exp[-1/J_{df}N(E_F)]$, where $N(E_F)$ represents the density of states on the Fermi energy and is less sensitive to pressure than J_{df}. On the contrary, the uniaxial pressure along the a axis should decrease J_{df} and hence T_K. These expectations are qualitatively consistent with the present observation. Especially, similar behavior observed for the cases of $P_u \parallel c$ axis and hydrostatic pressure experiments are naturally explained as a consequence of the similar pressure dependencies of $d_{\rm Ce-Ru}$.

The large anisotropy in the magnetic susceptibility in $CeRu_2Si_2$ is ascribed to the crystalline electric field (CEF) effect. At ambient pressure, the anisotropy

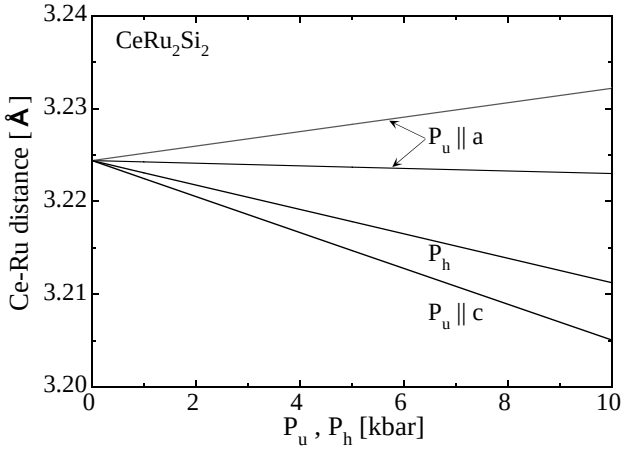

FIG. 6: Estimated change of Ce-Ru distance in $CeRu_2Si_2$ with uniaxial and hydrostatic pressure using the values of elastic constants (Ref. 14). The solid lines are guides to the eyes.

$\chi_{H\|c}/\chi_{H\|a} \sim 15$ at 4.2 K suggests the ground state is $a|\pm\frac{5}{2} - \sqrt{(1-a^2)}|\mp\frac{3}{2}\rangle$, $a \sim 0.96$.[9] The maximum anisotropy in the magnetic susceptibility is expected for a CEF ground state of pure $|\pm\frac{5}{2}\rangle$. $\chi_{H\|c}$ is largely suppressed, while $\chi_{H\|a}$ is slightly enhanced by $P_u \parallel c$ axis. Therefore, the anisotropy $\chi_{H\|c}/\chi_{H\|a}$ decreases with increasing $P_u \parallel c$ axis. This may reflect a change of the CEF ground state, i.e., an increase of the $|\mp\frac{3}{2}\rangle$ component in the ground state by $P_u \parallel c$ axis. For the Ce^{3+} ion, the charge distribution of $|\mp\frac{3}{2}\rangle$ is dumbbell shaped with its elongation along the c-axis[17]. Moreover in the $CeRu_2Si_2$ crystal unit cell, the Ru atom is located at $(0,\frac{1}{2},\pm\frac{1}{4})$ with respect to the Ce ion.[16] Therefore, besides the decrease of Ce-Ru distance, an increase of the $|\mp\frac{3}{2}\rangle$ component also consistently favors the strong enhancement of Ce-Ru hybridization by $P_u \parallel c$ axis. It is argued that there is an anomalous peak structure in the partial density of the hybridized-band state (the DOS) due to anisotropic hybridization between $4f$ and conduction electrons in the case where the lowest CEF level is $|\pm\frac{5}{2}\rangle$.[3,9] In this case, the anisotropic hybridization has an angular dependence characterized by $(1-\hat{k}^2{}_z)^2$. The differential susceptibility diverges when the peak in the DOS crosses the Fermi level giving rise to the metamagnetic anomaly at H_M. As discussed in the previous section comparing the transverse MR under $P_u \parallel c$ axis with the reported MR behavior under hydrostatic pressure, the decrease and broadening of the ρ peak at $H_{\max}$ may suggest a change of DOS with $P_u \parallel c$ axis. A possible change of the CEF ground state, i.e., an increase of the $|\mp\frac{3}{2}\rangle$ component by $P_u \parallel c$ axis may cause a decrease and broadening of the anomalous peak in the DOS near the Fermi level predicted for anisotropic hybridization. It may be noted that for a pure $|\mp\frac{3}{2}\rangle$ ground state the DOS near the Fermi level has a finite value rather than a peak as shown in the case of the Kondo insulator CeNiSn[9,18]. In order to determine the quantitative change or broadening of the DOS, measurements of the field dependence of specific heat under uniaxial pressure are needed.

V. CONCLUSION

We have found that the uniaxial pressure has an anisotropic effect on the magnetic and transport properties in the heavy-fermion metamagnet $CeRu_2Si_2$ with a direct influence on the hybridization. The characteristic parameters $T_{\max}$, Θ_p, $\chi^{-1}_{T\simeq 0}$, and H_M roughly scale as the uniaxial pressure is varied, leading to a single-energy-scale picture, namely, the variation of T_K. The results suggest that T_K (or d-f hybridization) is strongly enhanced for the pressure along the c axis due to the decrease of the nearest Ce-Ru distance, while T_K is weakly suppressed for the pressure along the a axis due to the increase of Ce-Ru distance. The decrease of the anisotropy of magnetic susceptibility and the decrease and broadening of the magnetoresistance peak at the metamagnetic anomaly indicate a controlling of the anisotropic hybridization by uniaxial pressure.

ACKNOWLEDGMENT

The authors are grateful to thank Profs. E. V. Sampathkumaran, M. Kohgi, O. Sakai, M. Yoshizawa, Y. Uwatoko, and K. Miyake for their comments and help. This work has been partly supported by a Grant-in-Aid for Scientific Research from the Ministry of Education, Science, Sports, and Culture of Japan.

[1] P. Haen, J. Flouquet, F. Lapierre, P. Lejay, and G. Remenyi, J. Low. Temp. Phys. 67, 391 (1987).
[2] R.A. Fisher, C. Marcenat, N. E. Phillips, P. Haen, F. Lapierre, P. Lejay, J. Flouquet, and J. Voiron, J. Low Temp. Phys. 84, 49 (1991).
[3] Y. Aoki, T. D. Matsuda, H. Sugawara, H. Sato, H. Ohkuni, R. Settai, Y. Ōnuki, E. Yamamoto, Y. Haga, A. V. Andreev, V. Sechovský, L. Havela, H. Ikeda, and K. Miyake J. Magn. Magn. Mater. 177-181, 271 (1998).
[4] H. Aoki, S. Uji, A. K. Albessard, and Y. Ōnuki, Phys. Rev. Lett. 71, 2110 (1993).
[5] T. Sakakibara, T. Tayama, K. Matsuhira, H. Mitamura, H. Amitsuka, K. Maezawa, and Y. Ōnuki, Phys. Rev. B 51, R12 030 (1995).
[6] S. Kambe, J. Flouquet, P. Haen, and P. Lejay, J. Low Temp. Phys. 102, 477 (1996).

[7] J. Voiron, J.-M. Mignot, P. Haen, and J. Flouquet, J. Phys. (France) 49, 1555 (1988).
[8] J.-M. Mignot, A. Ponchet, P. Haen, F. Lapierre, and J. Flouquet, Phys. Rev. B 40, 10917 (1989); J.-M. Mignot, J. Flouquet, P. Haen, F. Lapierre, L. Puech, and J. Voiron, J. Magn. Magn. Mate. 76-77, 97 (1988), references therein.
[9] K. Hanzawa, K. Ohara, and K. Yosida, J. Phys. Soc. Jpn. 66, L3001 (1997); K. Ohara, K. Hanzawa, and K. Yosida, *ibid*. 68, 521 (1999).
[10] S. R. Saha, Ph. D. thesis, Tokyo Metropolitan University, 2001.
[11] Y. Uwatoko, J. L. Sarao, J. D. Thompson, N. Môri, and G. Oomi, Rev. High Pressure Sci. Technol. 7, 1508 (1998); H. Mori, N. Takeshita, N. Môri, Y. Uwatoko, Physica B 259-261, 58 (1999).
[12] L. D. Jennings and C. A. Swenson, Phys. Rev. 112, 31 (1958).
[13] T. F. Smith and C. W. Chu, Phys. Rev. 159, 353 (1967).
[14] D. Weber, Ph. D. thesis, Frankfurt University, 1991.
[15] T. Endstra, G. J. Nieuwenhuys, and J. A. Mydosh, Phys. Rev. B 48, 9595 (1993).
[16] H. Yamagami and A. Hasegawa, J. Phys. Soc. Jpn. 62, 592 (1993).
[17] U. Walter, Z. Phys. B: Condens. Matter 62, 299 (1986).
[18] H. Ikeda and K. Miyake, J. Phys. Soc. Jpn. 65, 1769 (1996).